Design Considerations of an Active Integrated Antenna with Negative Resistance Transistor Oscillator

Davor BONEFAČIĆ, Juraj BARTOLIĆ

Dept. of Radiocommunications, Faculty of Electrical Engineering and Computing, University of Zagreb,
Unska 3, 10 000 Zagreb, Croatia

davor.bonefacic@fer.hr, juraj.bartolic@fer.hr

Abstract. *The design of an active integrated antenna with negative resistance transistor oscillator has been described. Simple but reasonably accurate analysis of oscillation start-up and steady state operating frequency prediction is presented. The active antenna prototype was manufactured and its operating frequency, EIRP and radiation patterns were measured. Two of these antennas were integrated in active arrays coupled in E- and H-planes. The inter-element distance in the arrays was optimized to obtain in-phase operation and mutual injection locking. Very good power combining efficiency was measured and beam scanning capabilities were demonstrated for both arrays.*

Keywords

Antenna, microstrip antenna, active integrated antenna, antenna array, spatial power combining, electronic beam scanning.

1. Introduction

Although the concept of active integrated antennas and arrays is known for more than three decades the interest for them is still growing because of the advantages they offer. The compact antenna element integrated with an active device for power generation finds its applications in communications [1] and radar systems [2] because of small dimensions, fabrication simplicity, low weight and low cost. By integration of two or more active oscillating antennas in arrays new advantages as free space power combining [3], [4], [5] and beam scanning without phase shifters [6], [7] emerge.

When the power from multiple radiating sources is combined in free space the losses in combining circuits are avoided. To obtain power combining all array elements have to be mutually injection locked. Injection locking is realized through mutual coupling between the array elements. The coupling can be weak (mainly radiative [3], [4]) or strong (e.g. by using coupling lines [8], [9] or integrating oscillators in spatial grids [10]).

In this paper the design procedure of an active oscillating antenna with the oscillator circuit integrated inside an opening in the patch is presented. Furthermore, its applicability for building active arrays is demonstrated.

2. Oscillator Theory

When the active oscillating antenna is built, the active device or circuit is integrated with the microstrip radiator. The patch antenna as a resonant element determines the operating frequency of this oscillator. When designing a spatial oscillator with an one-port (e.g. Gunn device), the condition to be satisfied is suitable impedance matching between the active device and the radiating element [8]. When a two-port device (e.g. bipolar transistor or FET) is used there are two possibilities. The first is to load the two-port device in such a way to get negative resistance in the frequency band of interest at one of the ports. In that case the oscillator design is similar to the one with an one-port. The second possibility is to use the active two-port as an amplifier with positive feedback [11]. This approach usually requires relatively long lines to assure the required phase shift in the feedback loop resulting in larger substrate area for the fabrication of the active antenna. In this paper the first approach has been used because it allows the design of a compact active antenna suitable for integration in arrays with inter element spacing less than a wavelength.
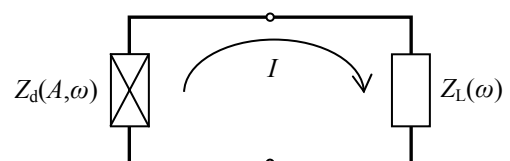

Fig. 1. Equivalent circuit of a negative resistance oscillator.

Every noise free negative resistance oscillator, independently of its actual composition, can be represented with the circuit shown in Fig. 1 [12]. Here $Z_d(A, \omega)$ is the impedance of the active device, $Z_L(\omega)$ is the impedance of the passive load, A is the amplitude of the current in the loop ($I = A \cdot e^{j\omega t}$), and ω is the angular frequency. The circuit in Fig. 1 is then described with:

$$\left[Z_d(A, \omega) + Z_L(\omega) \right] \cdot I = 0 \quad . \tag{1}$$

As the dependence of the active device impedance $Z_d(A, \omega)$

on the current amplitude A is predominant, the dependence on the angular frequency ω can be neglected. When the oscillations exist in the circuit, the current can not be zero ($I \neq 0$). As (1) is valid, the expression in square brackets must equal zero, which results in:

$$Z_L(\omega) = -Z_d(A) \quad . \tag{2}$$

Equation (2) must be satisfied in the circuit on Fig. 1 in steady state. In graphic interpretation equation (2) is the intersection point of the active device impedance locus $-Z_d(A)$ and load impedance locus $Z_L(\omega)$. However, the condition given by (2) is necessary but not sufficient for stable operating point of the oscillator [12]. In case that the loci of $Z_L(\omega)$ and/or $-Z_d(A)$ have one or more loops several intersections can exist resulting in one or more stable and unstable operating points.

Considering the design of an active integrated antenna, $Z_d(A)$ is the impedance at the output of the oscillator circuit and $Z_L(\omega)$ is the antenna input impedance.

3. The Modified Patch Antenna

The modified patch with the line transformer, similar to the one used in the design presented in this paper, was introduced in [13] where a Gunn device was used as the active element. However, it was shown that, due to the relatively large negative resistance bandwidth of the Gunn device, the oscillating antenna suffered from mode instabilities. The design presented in this paper uses a bipolar transistor as the active device. The bandwidth of its negative resistance can be better controlled which eliminates mode hopping.

The patch antenna was designed and optimized by using the IE3D electromagnetic simulator from Zeland Software, Inc. The rectangular patch was designed for operation in TM_{01} mode. The substrate had the height of 1.576 mm, relative dielectric constant of 2.55 and the loss tangent of 0.0019. A 10 mm × 25 mm rectangular opening has been made symmetrically inside the patch to allow the placing of the transistor and the impedance matching network. The rectangular opening lowered the patch resonant frequency. This was compensated by reducing the patch resonant dimension l (Fig. 2). Finally, the patch dimensions were $w = 42.3$ mm and $l = 34.7$ mm. The opening dimensions were determined by two opposite requirements: to have enough space for placing the oscillator circuit and the impedance matching network and to maintain the patch intact as much as possible in order to reduce the disturbance of the current distribution on the patch and to assure the excitation of the antenna in TM_{01} mode. Furthermore the opening dimensions must not be resonant and it must not radiate. The calculated current distribution (Fig. 2) on the modified patch and the measured radiation patterns confirm that this modification has not significantly altered the current distribution on the patch. To reduce the cross-polarization levels it is the best to excite the patch at its line of

symmetry. Two of the opening edges are close to the patch radiating edges, so the input impedance at resonance at this points will be quite high (approx. 200 Ω). This was confirmed by simulation. Relatively high impedance at the center of the opening edge has to be transformed to lower impedance which satisfies the conditions for starting of the oscillations [12]. A suitable impedance transformation has been achieved with a 5 mm × 13.7 mm microstrip line.

Furthermore, the locus of the antenna input impedance should not have loops in the bandwidth where the active circuit will show negative resistance to assure stable operation of the active integrated antenna. This issue will be further discussed in the next section.
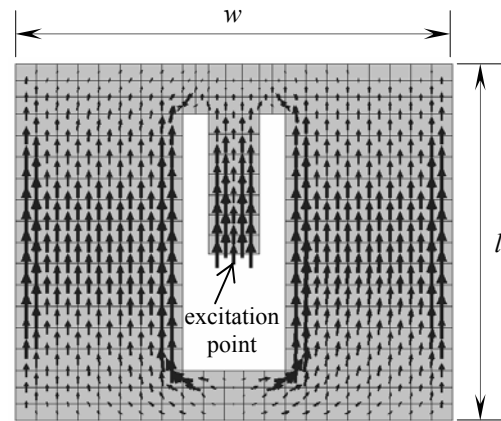

Fig. 2. Calculated current distribution on the modified patch at resonance (2.3 GHz).

4. The Oscillator

The active device in the oscillator is the Hewlett-Packard AT-41485 NPN bipolar transistor in common collector configuration (Fig. 3).
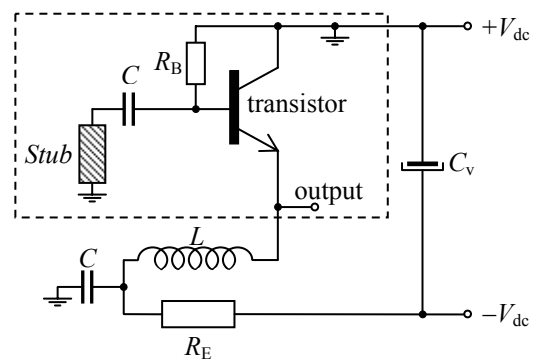

Fig. 3. Transistor oscillator circuit.

The common collector configuration is used because it allows simple biasing network and offers very good possibility to control the negative resistance bandwidth at the oscillator output. The length and the characteristic impedance of the destabilizing inductive short-circuited stub (*Stub* in Fig. 3), which is connected to the transistor base terminal, were optimized to obtain negative resistance at

the emitter in the frequency band around 2.3 GHz. The emitter terminal is used as the oscillator output and it is connected to the patch antenna. The resistor R_B connected from the collector to the base provides the base dc biasing. The dc biasing of the emitter is realized by negative dc voltage connected through a high-impedance microstrip line to the center of the patch non-radiating edge while the positive dc voltage is connected to the ground plane. The dc blocking capacitors are marked with C, R_E is the emitter resistor and the capacitor C_v filters eventual fluctuations of the dc source. The inductor L is used as RF choke. Only the elements included in the dashed rectangle in Fig. 3 are embedded in the opening inside the patch.
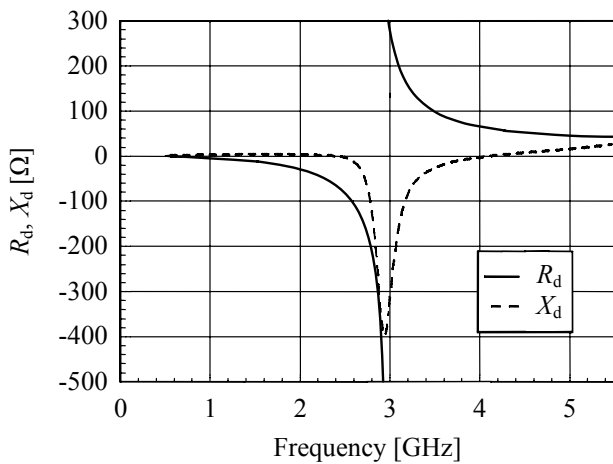

Fig. 4. Calculated real (R_d) and imaginary (X_d) part of the impedance at the output of the oscillator in Fig. 3.

The calculated impedance with a negative real part ($Z_d = R_d + j X_d$) at the oscillator output (Fig. 3) is shown in Fig. 4. This impedance is obtained by using the small signal scattering parameters given by the transistor manufacturer [14]. These results are important for examining conditions at the oscillation start-up. In Fig. 4 it can be seen that negative resistance at the oscillator output port exists in the bandwidth from 600 MHz to 2.93 GHz.

The operation of the active integrated antenna will be stable if the active circuit loaded with the input impedance of the microstrip antenna satisfies the conditions for stable operation [12]. The interaction between the modified microstrip patch (Fig. 2) and the oscillator circuit (Fig. 3) can be analyzed graphically. Fig. 5 shows the calculated antenna input impedance $Z_L(\omega)$ and its possible intersections with negative of the active device impedance loci $-Z_d(A)$. It can be seen that other loops in the $Z_L(\omega)$ locus will be formed at frequencies below 500 MHz or above 3 GHz where there is no negative resistance at the oscillator output. This implies that there will be only one stable operating point of the oscillator.

The magnitudes and phases of all four transistor scattering parameters change with the increase of oscillation amplitude. This should be taken into account in rigorous analysis of the oscillator behavior. However, simplified analysis and approximate estimation of the system behavior

can be made considering only the decrease of the magnitude of the transistor s_{21} parameter. In this way the loci of the negative of the active device impedance $-Z_d(A)$ in Fig. 5 have been obtained. These loci are derived for five frequencies between 2.1 GHz and 2.5 GHz, with a step of 100 MHz. The arrows on $-Z_d(A)$ curves indicate the direction of the increasing oscillation amplitude. The oscillator operating point in steady state is determined by the intersection of the $-Z_d(A)$ and $Z_L(\omega)$ loci. In Fig. 5 it can be observed that the intersection of the $-Z_d(A)$ curve for 2.3 GHz with the impedance locus $Z_L(\omega)$ occurs very close to the 2.3 GHz frequency point of on the $Z_L(\omega)$. Therefore equation (2) will be satisfied at this frequency. This shows that even such simple simulation can predict the operating frequency with reasonable accuracy.
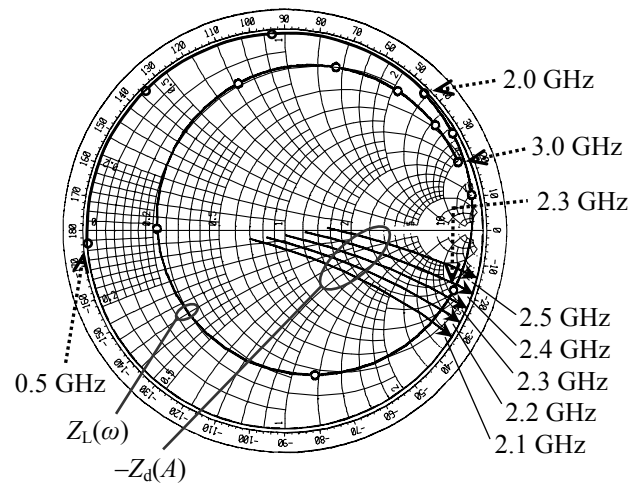

Fig. 5. Load impedance (patch input impedance) $Z_L(\omega)$ in the frequency band 0,5 ÷ 3 GHz (markers at every 500 MHz in the band 0,5 ÷ 2 GHz and at every 100 MHz in the band 2 ÷ 3 GHz) and the negative of the oscillator output impedance $-Z_d(A)$ for the frequencies 2.1; 2.2; 2.3; 2.4 and 2.5 GHz.

The oscillator circuit from Fig. 3 was adapted for integration inside the opening in the patch. The final layout of the active integrated antenna is shown in Fig. 6.
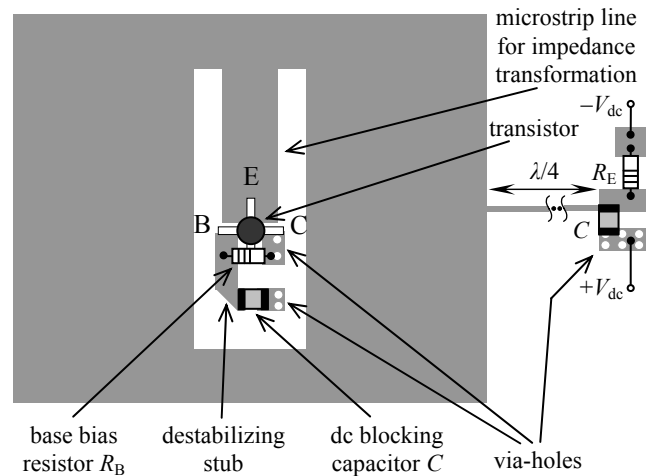

Fig. 6. Active integrated antenna layout.

The RF choke (inductor L) from Fig. 3 is replaced by a quarter wavelength long high-impedance microstrip line terminated by an RF short circuit (capacitor C connected between the end of the line and the ground plane, Fig. 6). For the dc voltage this point is isolated from the ground plane and here is connected the resistor R_E. On the other end of the resistor R_E is applied the negative dc voltage.

The low impedance (ideally short circuit) for RF signal obtained by the capacitor C connected to the ground plane is transformed by a quarter wavelength long microstrip line to high impedance (ideally open circuit) for RF signal at the patch non-radiating edge. In this way the dc bias circuit is decoupled from the antenna and the oscillator circuit.

5. Spatial Power Combining Arrays

Two active patches, described in the former section (Fig. 6), were integrated in two arrays, one coupled in E-plane (Fig. 7a) and the other in H-plane (Fig. 7b).
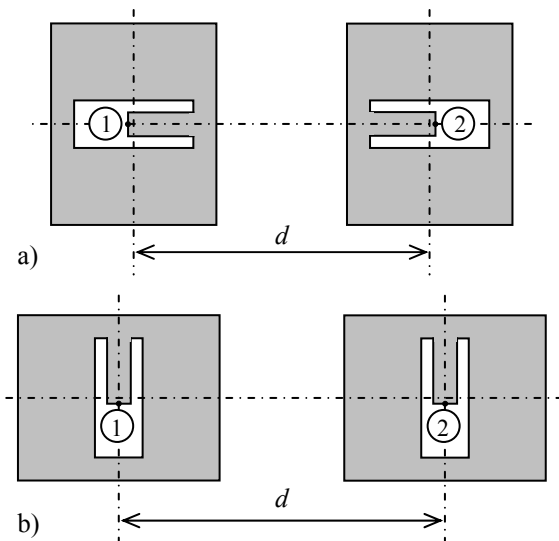

Fig. 7. Two-element arrays of active patches: a) coupled in E-plane, b) coupled in H-Plane (①, ② = excitation ports).

The two active integrated antennas are mutually coupled predominantly by radiation which results in mutual injection locking. The coupling strength and phase are determined by the array inter-element distance d. The analysis and stability considerations in [7] show that the coupling phase around 0° gives the best results for weakly coupled spatial power combining arrays. With the coupling coefficient phase of 0° and all elements adjusted to operate at the same free-running frequency, maximum power combining is obtained in the direction perpendicular to the plane of the array. Therefore, the inter element distance d is optimized for coupling coefficient phase of 0°. For the E-plane array (Fig. 7a) the array element orientation introduces an additional phase shift of 180°, and this has to be compensated by the coupling coefficient phase of 180°.

The inter-element distances and with it the coupling coefficient phases for both arrays have been optimized by the IE3D electromagnetic simulator package. The results are given in Table 1. The inter-element distance is given in terms of free space wavelength λ_0. The magnitude and phase of the coupling coefficient are calculated at 2.3 GHz.

Coupling plane	Inter-element distance d	Coupling coefficient phase	Coupling coefficient magnitude [dB]
E	$0.72\,\lambda_0$	180°	−39
H	$0.85\,\lambda_0$	0°	−45

Tab. 1. Optimization results for the active arrays.

6. Experimental Results

To verify the design considerations in the previous sections, two prototypes of the active integrated antenna were manufactured and their characteristics were investigated. Very good agreement of the measured results between the two active antennas was observed, thus the measurement results for only one antenna are given. Also the measurement results for E-plane coupled and H-plane coupled active spatial power combining arrays are given.

6.1 Active Integrated Antenna

As the microstrip radiator and the oscillator circuit are integrated together, the most appropriate way to characterize the output power of this system is to measure its equivalent isotropically radiated power ($EIRP$). The $EIRP$ is the product of the antenna gain and the oscillator output power when it is loaded with the antenna input impedance. The $EIRP$ is obtained by measuring the power P_r received by a calibrated measurement antenna with gain G_r at a known distance R from the tested active integrated antenna:

$$EIRP = \frac{P_r}{G_r} \cdot \left(\frac{4\pi R}{\lambda} \right)^2 \quad . \tag{3}$$

Here λ is the wavelength of the measured signal. The distance R should be large enough so that the received power P_r is measured in the far-field region [15].

The measured changes of the equivalent isotropically radiated power ($EIRP$) and the oscillating frequency in dependence of the dc bias voltage are shown in Fig. 8. By changing the dc bias from 2 to 9 V a frequency tuning range of about 40 MHz was obtained. It can be seen that the change of the oscillating frequency with the bias voltage is very linear. At 9 V bias the discrepancy from the design frequency of 2.3 GHz is less than 0.5%. At the same bias voltage of 9 V the maximal EIRP of 19.4 dBm was measured and a dc to RF conversion efficiency of 33% was obtained. This oscillating antenna showed stable operation and clean spectrum in the whole frequency tuning range.
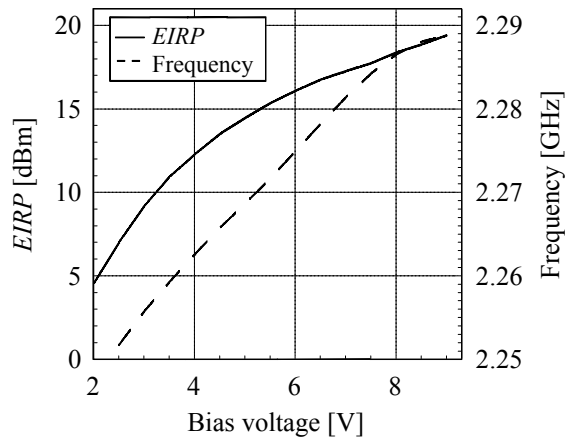
Fig. 8. Measured *EIRP* and frequency as functions of bias voltage.

The measured E- and H-plane radiation patterns are shown in Fig. 9. The co-polarization radiation patterns in both E- and H-planes are symmetrical around broadside and they are not affected by the patch modifications and electronic circuits inside the antenna. The cross-polarization levels are below –23.2 dB in E-plane and bellow –17.7 dB in H-plane for all angles.
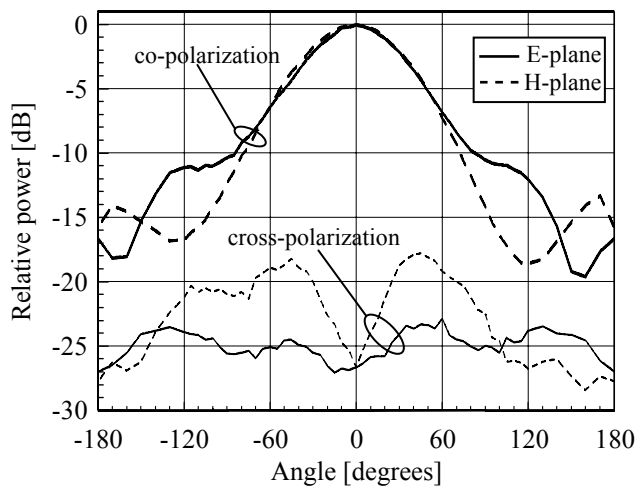

Fig. 9. Measured E-plane (solid) and H-plane (dashed) co-polarization (thick line) and cross-polarization (thin line) radiation patterns of the active patch.

The measured spectrum of this active antenna was clean and the operation was stable. The content of the second harmonic in the radiated signal in the broadside direction was measured. The highest measured level of the second harmonic was observed at 9 V bias and its level was 35.2 dB bellow the fundamental. The results for other bias voltages are given in Table 2. The levels of harmonic components of the order higher than two were below the noise floor of the measuring instrument.

6.2 Two-Element Active Arrays

The array spatial power combining efficiency is calculated from the measured radiated power in the case of

broadside radiation divided by the array factor and by the sum of powers radiated by each array element in the free running conditions. The results are given in Table 3.

Bias voltage [V]	Second harmonic level with respect to fundamental [dB]
5	–40.5
7	–37.3
9	–35.2

Tab. 2. Measured levels of the second harmonic in the radiated signal.

The E-plane array showed power combining efficiency of 105 %. A combining efficiency larger than 100 % can be explained by better impedance matching between the oscillator circuit and the patch antenna obtained in the array due to the interaction between the array elements. Another reason for combining efficiency larger than 100 % can be the increase of the power radiated by each of the array elements in injection locking conditions [12].

Coupling plane	Power combining efficiency	Beam scanning range	Max cross-polar levels [dB] broadside / left sc./ right sc.
E	105 %	±17°	–22 / –21 / –20
H	97 %	±11°	–20 / –19 / –20

Tab. 3. Measurement results for the active arrays.

Beam scanning is achieved by changing the bias voltage of one of the array elements. For both arrays symmetrical beam scanning around broadside has been obtained. The measured beam scanning ranges for both arrays were smaller than the theoretical maximum for given inter-element distance and maximal inter-element phase shift of ±90° (determined by the injection locking condition), because the operation near the edge of the locking bandwidth is unstable.

Fig. 10. Measured co-polarization (thick line) and cross-polarization (thin line) radiation patterns for E-plane array; broadside (solid); left scan (dashed); right scan (dotted).

Co-polarization and cross-polarization radiation patterns

have been measured for broadside radiation and for both maximal obtainable scanned positions of the main beam (Figs 10 and 11). The maximal measured cross-polarization levels for broadside radiation as well as for both scanned beam positions are given in Table 3.
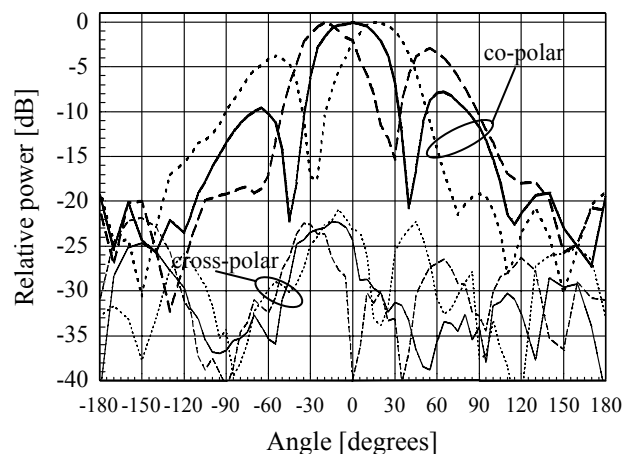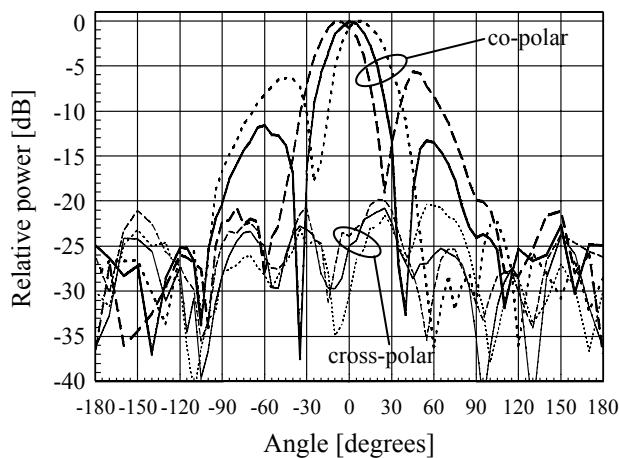

Fig. 11. Measured co-polarization (thick line) and cross-polarization (thin line) radiation patterns for H-plane array; broadside (solid); left scan (dashed); right scan (dotted).

The measured spectra of both arrays were clean and stable. A slight increase of the noise in the spectrum was observed in the two scanned positions of the main beam. The increase of the noise in the scanned positions is due to the operation close to the end of the injection locking range.

7. Conclusion

An active integrated antenna built by integrating a negative resistance transistor oscillator and a line impedance transformer in a rectangular opening inside a rectangular patch has been presented. This compact and low cost design showed very linear change of the oscillating frequency with the dc bias voltage. A clean spectrum was observed in the whole frequency tuning range. The radiation patterns showed no degradation in comparison to a non-modified patch. The cross-polarization levels in both E- and H-planes were low.

This active oscillating patch antenna has been used as a building component for two two-element power combining active arrays, one coupled in E-plane and the other coupled in H-plane. The IE3D electromagnetic simulator package has been used to optimize the distance between the array elements in order to obtain the desired phase of the coupling coefficient for in-phase operation and mutual injection locking.

Both arrays showed very good spatial power combining efficiency. Symmetrical electronic beam scanning around broadside was demonstrated for both arrays. Beam scanning was achieved by changing the dc bias voltage of one of the spatial oscillators in the array. In both cases stable operation has been obtained for all scanned positions of the main beam. The measured spectra were clean. A slight increase of

the noise in the spectrum, measured in the cases of scanned beam positions, was observed. Measured cross-polarization levels were low.

References

[1] KYKKOTIS, C., HALL, P.S., GHAFOURI-SHIRAZ, H. Performance of active antenna oscillator arrays under modulation for communication systems. *IEE Proceedings - Microwaves, Antennas and Propagation*, 1998, vol. 145, no. 4, p. 313-320.

[2] MORROW, I.L., HALL, P.S., JAMES, J.R. Measurement and modeling of a microwave active-patch phased array for wide-angle scanning. *IEEE Transactions on Antennas and Propagation*, 1997, vol. 45, no. 2, p. 297-304.

[3] YORK, R.A., COMPTON, R.C. Quasi-optical power combining using mutually synchronized oscillator arrays. *IEEE Transactions on Microwave Theory and Techniques*, 1991, vol. 39, no. 6, p. 1000-1009.

[4] MURATA, M., MATSUI, T. 2×2 spatial power combining array of planar radiating oscillator using butterfly-shaped patch element. In *Proceedings of the 29th European Microwave Conference*. Munich (Germany), 1999, vol. 2, p. 201-204.

[5] CHANG, K., SUN, C. Millimeter-wave power-combining techniques. *IEEE Transactions on Microwave Theory and Techniques*, 1983, vol. MTT-31, no. 2, p. 91-107.

[6] BARTOLIĆ, J., BONEFAČIĆ, D., ŠIPUŠ, Z. Modified rectangular patch array with electronic beam scanning. In *Proceedings of the 14th International Conference on Applied Electromagnetics and Communications (ICECOM'97)*. Dubrovnik (Croatia), 1997, p. 67-70.

[7] YORK, R.A. Nonlinear analysis of phase relationships in quasi-optical oscillator arrays. *IEEE Transactions on Microwave Theory and Techniques*, 1993, vol. 41, no. 10, p. 1799-1809.

[8] LIN, J., ITOH, T. Two-dimensional quasi-optical power-combining arrays using strongly coupled oscillators. *IEEE Transactions on Microwave Theory and Techniques*, 1994, vol. 42, no. 4, p. 734-741.

[9] RAHMAN, M., IVANOV, T., MORTAZAVI, A. A 26-MESFET spatial power-combining oscillator. *IEEE Microwave and Guided Wave Letters*, 1997, vol. 7, no. 4, p. 100-102.

[10] WEIKLE, II, R.M. et al. Planar MESFET grid oscillators using gate feedback. *IEEE Transactions on Microwave Theory and Techniques*, 1992, vol. 40, no. 11, p. 1997-2003.

[11] MARTINEZ, R.D., COMPTON, R.C., High-efficiency FET/microstrip-patch oscillators. *IEEE Antennas and Propagation Magazine*, 1994, vol. 36, no, 1, p. 16-19.

[12] KUROKAWA, K., Injection locking of microwave solid-state oscillators. *Proceedings IEEE*, 1973, vol. 61, no. 10, p. 1386-1410.

[13] BARTOLIĆ, J., BONEFAČIĆ, D., ŠIPUŠ, Z. Modified rectangular patches for self-oscillating active antenna applications. *IEEE Antennas and Propagation Magazine*, 1996, vol. 38, no, 4, p. 13-21.

[14] –, *AT-41485, Up to 6 GHz Low Noise Silicon Bipolar Transistor – Technical Data*. Hewlett-Packard Co., USA, 1997.

[15] BALANIS, C.A. *Antenna Theory: Analysis and Design*. 2nd ed. New York: John Wiley, 1997.

About Authors...

Davor BONEFAČIĆ was born in Zagreb, Croatia, in 1968. He received his Dipl.Ing., Mr.Sc. and Dr.Sc. degrees from the Faculty of Electrical Engineering and Computing, University of Zagreb in 1993, 1996, and 2000, respectively. Since 1993, he has been with the Department of Radio-

communications and Microwave Engineering, Faculty of Electrical Engineering and Computing, University of Zagreb. From 1993 to 2002 he worked as a research assistant. Currently he is Assistant Professor at the same Department. His teaching activity includes several subjects on microwave engineering and radar systems. In 1996 he was a visiting researcher at the Third University of Rome, Rome, Italy. In 1996 he was awarded with the silver plaque "J. Lončar" for outstanding master thesis. Since 2004 he is a collaborating member of the Croatian Academy of Engineering. He is co-author of more than 50 journal articles and conference papers. Besides teaching and research his professional activity includes measurement of field distribution and estimation on health risk of mobile communication base stations and radar installations, technical inspections of radio broadcasting stations, and calibration and conformity verification of RF measurement equipment. His research interests include active integrated antennas and arrays, spatial power combining, electronic beam scanning, small and compact antennas for wireless communications, and wideband antennas.

Juraj BARTOLIĆ was born in Zagreb, Croatia, in 1948. He received the Dipl. Ing., M.S., and Ph.D. degrees in electrical engineering from the University of Zagreb in 1971, 1975, and 1982, respectively. From 1972 to 1974 he worked for the Radio Industry of Zagreb in R&D of microwave radio. In 1974, he joined the Institute for High Frequency Techniques, Faculty of Electrical Engineering at the University of Zagreb, were he was a Research Assistant, Assistant Professor, and Associate Professor. Currently, he is a Professor in the Department of Radiocommunications and Microwave Engineering, Faculty of Electrical Engineering and Computing, University of Zagreb. He served as Head of the Department from 2000 to 2004. Since 1998 he is a member of the Croatian Academy of Engineering. He is the co-author of the book Mixing, Mixers, and Frequency Synthesizers, and the author and co-author of more then 150 technical papers in journals and conferences. His research interests include electromagnetics, antennas and propagation, wireless circuit design, microwave engineering, and electromagnetic compatibility (EMC). He is a Senior Member of IEEE.

RADIOENGINEERING REVIEWERS
December 2005, Volume 14, Number 4

- ALÚ, A., Universitá di Roma Tre
- BILÍK, V., Slovak Univ. of Technology, Bratislava
- BONEFAČIĆ, D., University of Zagreb
- ČERNOCKÝ, J., Brno University of Technology
- ČERNOHORSKÝ, D., Brno Univ. of Technology
- DĚDKOVÁ, J., Brno University of Technology
- DOBOŠ, L., Technical University of Košice
- DOSTÁL, T., Brno University of Technology
- FIŠER, O., Czech Academy of Sciences, Praha
- FONTÁN, F. P., University of Vigo
- FRÝZA, T., Brno University of Technology
- FUČÍK, O., Brno University of Technology
- HÁJEK, K., University of Defense, Brno
- HALÁMEK, J., Czech Academy of Sciences, Brno
- HANUS, S., Brno University of Technology
- HOZMAN, J., Czech Technical Univ., Prague
- HRABAR, S., University of Zagreb
- JAN, J., Brno University of Technology
- KASAL, M., Brno University of Technology
- KOZUMPLÍK, J., Brno University of Technology
- KVIČERA, V., TESTCOM, Praha
- LÁČÍK, J., Brno University of Technology
- LUKEŠ, Z., Brno University of Technology
- MACHÁČ, J., Czech Technical University, Prague
- MARŠÁLEK, R., Brno University of Technology
- MAZÁNEK, M., Czech Technical Univ., Prague
- NOVÁČEK, Z., Brno University of Technology
- POLÍVKA, M., Czech Technical Univ., Prague
- POUPA, M., Univ. of Western Bohemia, Pilsen
- PROKEŠ, A., Brno University of Technology
- RAIDA, Z., Brno University of Technology
- SCUCCHIA, L., Universitá di Roma Tor Vegata
- SCHEJBAL, V., University of Pardubice
- SOKOL, V., Czech Technical University, Prague
- SVAČINA, J., Brno University of Technology
- ŠKVOR, Z., Czech Technical University, Prague
- TKADLEC, R., Brno University of Technology
- URBANEC, T., Brno University of Technology
- VOREL, P., Brno University of Technology
- ZAVACKÝ, J., Technical University of Košice